

Liquid-hexatic-solid phase transition of a hard-core lattice gas with third neighbor exclusion

Cite as: J. Chem. Phys. **151**, 104702 (2019); <https://doi.org/10.1063/1.5123231>

Submitted: 03 August 2019 . Accepted: 14 August 2019 . Published Online: 10 September 2019

Shaghayegh Darjani , Joel Koplik , Sanjoy Banerjee, and Vincent Pauchard



[View Online](#)



[Export Citation](#)



[CrossMark](#)

Lock-in Amplifiers up to 600 MHz

starting at
\$6,210



 **Zurich
Instruments**

[Watch the Video](#) 

Liquid-hexatic-solid phase transition of a hard-core lattice gas with third neighbor exclusion

Cite as: J. Chem. Phys. 151, 104702 (2019); doi: 10.1063/1.5123231

Submitted: 3 August 2019 • Accepted: 14 August 2019 •

Published Online: 10 September 2019



View Online



Export Citation



CrossMark

Shaghayegh Darjani,^{1,2} Joel Koplik,^{3,a} Sanjoy Banerjee,¹ and Vincent Pauchard¹

AFFILIATIONS

¹Energy Institute and Department of Chemical Engineering, City College of New York, New York, New York 10031, USA

²Benjamin Levich Institute and Department of Chemical Engineering, City College of the City University of New York, New York, New York 10031, USA

³Benjamin Levich Institute and Department of Physics, City College of New York, New York, New York 10031, USA

^ajkoplik@ccny.cuny.edu

ABSTRACT

The determination of phase behavior and, in particular, the nature of phase transitions in two-dimensional systems is often clouded by finite size effects and by access to the appropriate thermodynamic regime. We address these issues using an alternative route to deriving the equation of state of a two-dimensional hard-core particle system, based on kinetic arguments and the Gibbs adsorption isotherm, by the use of the random sequential adsorption with a surface diffusion model. Insight into coexistence regions and phase transitions is obtained through direct visualization of the system at any fractional surface coverage via local bond orientation order. The analysis of the bond orientation correlation function for each individual configuration confirms that first-order phase transition occurs in a two-step liquid-hexatic-solid transition at high surface coverage.

Published under license by AIP Publishing. <https://doi.org/10.1063/1.5123231>

I. INTRODUCTION

The phase behavior of the two dimensional systems is a key aspect of many current research areas such as emulsion stability due to particle adsorption at the interface,^{1,2} particle self-assembly into clusters,^{3–6} chemisorption on metal surface,^{7,8} and melting at an interface.^{9,10} Numerous equations of state (EOS) such as the Langmuir¹¹ and Volmer models have been introduced over the years to describe the adsorption behavior of such systems.^{12,13} The Langmuir model is based on localized adsorption where the adsorbate molecules are smaller than the adsorption sites,¹⁴ but in many practical cases, the adsorbate is actually larger than the adsorption site. Likewise, the Volmer model, which assumes fully delocalized adsorption (adsorbates much bigger than the adsorption sites), is equally inappropriate except, perhaps, for nanoparticles. Rather than directly prescribing the EOS, an alternative is the random sequential adsorption model (RSA), which describes the dynamics of the adsorption process by allowing objects to adsorb sequentially

onto the open sites of a one- or two-dimensional lattice.¹⁵ The model has been extensively used in the literature, for example by Manzi *et al.*¹⁶ who discuss the adsorption of human serum albumin on the nanostructure of a black silicon surface using RSA. Further applications of this model include chemisorption, deposition, layered growth, vibrated granular material, and the car-parking problem.^{17–26}

More specifically, in the RSA model, molecules or particles are progressively added at random to an initially empty surface with the only restriction that overlap is not allowed, an assumption based physically on short-range electrostatic repulsion. As the coverage increases, the free area left for further adsorption decreases, not only because the sites are occupied by previously adsorbed molecules but also because vacancies can be too small to allow adsorption without overlap. Without desorption or surface diffusion, adsorption kinetics rapidly slows down and coverage asymptotically approaches the jamming limit (equivalent to maximum random packing) if the substrate is not prepatterned. However, it has experimentally been

observed²⁷ that the relaxation time scale of adsorbed particles, due to their rearrangement on the surface, can be comparable to the deposition time scale. The final configuration is comparable with a dense-packed ordered system. Furthermore, none of the above models is able to explain the ordered layering observed in adsorption of certain materials on the surface.^{7,8,27}

A different approach is taken in the lattice gas model, which uses statistical mechanical reasoning to describe adsorbate configurations on a surface, where an adsorbate molecule may occupy one or a few adsorption sites. Applications of this model include a recent study of photoexcited Rydberg gases by Ji *et al.*,²⁸ where an order-disorder phase transition corresponds to the phase transition on a square lattice with first neighbor exclusion, a study of self-assembly of isophthalic acid on graphite by Lackinger *et al.*,²⁹ adsorption of selenium on nickel surface by Bak *et al.*⁷ and chemisorption of oxygen on palladium by Zhang *et al.*³⁰ Although the lattice gas model has been studied extensively in the literature, only the single case of a triangular lattice with first neighbor exclusion was solved exactly, by Baxter.³¹ For all other variants, a number of lattice gas methods have been developed over years based on various approximation methods: the matrix method of Kramer and Wannier,^{32–38} the density (or activity) series expansion method,^{32,33,39–43} the generalized Bethe method,^{44–46} Monte Carlo simulation,^{37,47–51} the Rushbrooke and Scoins method,⁵² and fundamental measure theory.⁵³ Despite all of this effort, the lattice gas model is not able to describe the adsorption isotherm of the system and instead focuses on the equation of state and the nature of phase transition.

In order to combine the advantages of both the RSA and lattice gas models, we previously developed an alternative route to deriving the equation of state of a two-dimensional hard-core particle with first neighbor exclusion, based on kinetic arguments and the Gibbs adsorption isotherm: the RSAD model.⁵⁴ Here, one considers a two-dimensional lattice gas in equilibrium with a three-dimensional solution of adsorbate molecules, where the equality of chemical potential throughout the system leads to

$$d\Pi = kT \frac{\Theta}{A_a} d\ln C, \quad (1)$$

where A_a is the interfacial area covered by a single adsorbate molecule, θ is the fractional surface coverage, and C is the concentration of the (three-dimensional) solution. Integrating the above equation gives

$$\int_0^\Theta \frac{\Theta}{C} \frac{\partial C}{\partial \Theta} d\Theta = \frac{A_a}{kT} \Pi, \quad (2)$$

from which we see that knowledge of the adsorption isotherm, the relationship between $C(\Theta)$, bulk concentration, and fractional coverage, enables one to calculate the equation of state $\Pi(\Theta)$.

The adsorption isotherm, in turn, can be obtained through kinetic arguments. At equilibrium, the rates of adsorption and desorption of molecules are equal,

$$K_a C(1 - \beta(\Theta)) = K_d \Theta, \quad (3)$$

where K_a and K_d are the adsorption and desorption rate constants, respectively, and $\beta(\Theta)$ is the “blocking function,” the fraction of the

surface area which is excluded from further adsorption by already adsorbed molecules. Solving for C and inserting the result into the integral version of the Gibbs adsorption isotherm yield

$$\int_0^\Theta (1 - \beta(\Theta)) \frac{\partial}{\partial \Theta} \left[\frac{\Theta}{1 - \beta(\Theta)} \right] d\Theta = \frac{A_a}{kT} \Pi. \quad (4)$$

Thus, the blocking function is the only information needed to calculate the equation of state, and we have shown previously⁵⁴ that for lattice gases, the blocking function can be easily extracted from RSAD model simulations.

In the RSAD model, where surface diffusion is introduced in parallel with adsorption, vacancies large enough to adsorb a further particle are both created and destroyed. When diffusion is sufficiently rapid, the size distribution of vacancies no longer depends on the history of adsorption (the positions where the adsorbates first arrived on the substrate) but only on the fractional surface coverage. One of the advantages of using the RSAD model is in locating the equilibrium state, which assures us that enough thermalization is present to reach the equilibrium state. Note that in this model, the potential energy is effectively infinite for particle overlap, due to the repulsive interaction, which restricts the occupancy of neighbors, and is zero otherwise. The system can therefore be considered as athermal.^{38,50,54} Our results show that the RSAD model can be used as an equilibrium model and our equation of state, the nature of our phase transition, and the phase transition coverage are in excellent agreement with the only model with an exact solution in the literature.³¹ From the definition of the adsorption rate, used above to define adsorption equilibrium, the blocking function can be extracted from the numerical simulations through the derivative of surface coverage with respect to the number of attempts,

$$\frac{\partial N}{\partial n} = 1 - \beta(\Theta). \quad (5)$$

Here, N is the number of adsorbed molecules, n is the number of attempts and t , defined by $nA_a/A = K_a C/t$, is an adimensional time defined via the adsorption rate. The latter definition will be used in practice by equating the blocking function to the rebuttal rate of adsorption attempts. Ushcats *et al.*⁴³ used an alternative method based on the power of activity at low and high densities, which shows the importance of accounting for the holes in deriving the equation of state of lattice gases. Based on their method,^{42,43} hole-particle symmetry, the total interaction energy is directly related to the interaction of holes at any specific configuration.

In this paper, we study the phase behavior of hard-core molecules with third neighbor exclusion on a triangular lattice and compare our results with those of Orban and Bellemans³³ who studied this model previously. Hard-core molecules with extended exclusion ranges are studied extensively in the literature but mainly on a square lattice.^{37,38,50,51,55–59} In some experiments, it is observed that lateral interactions of adsorbed particles on solid surfaces (chemisorption) follow the extended exclusion range, which is important in surface science as ordering affects the surface functionality.^{7,8,30,60} Increasing the exclusion range could also correspond to a smaller lattice site which becomes equivalent

to the continuum limit when the exclusion range is significantly large.^{33,50,51}

Simulation data related to the triangular lattice with third neighbor exclusion are given in Sec. III, where a first order liquid-hexatic-solid phase transition is obtained at high surface coverage. In the liquid state, positional and orientational correlations of particles decay exponentially, while in solid state, they have a quasi-long-range orientational order. Besides these two phases, there is an intermediate hexatic phase, where particles have quasi-long range orientational order and exponential positional order. We quantify the ordering using a bond orientation correlation function, $g_6(r)$, calculated from the local bond orientation order, $\Psi(r)$. In a dense system, most of the particles are surrounded by six particles, and the local bond orientation is represented by the sixfold orientation,

$$\Psi(r_j) = \frac{1}{N_k} \sum_{k=1}^{N_k} e^{i\theta_{jk}}, \quad (6)$$

where k is the number of the nearest neighbors of particle j and θ_{jk} is the angle between the line joining the centers of mass of particles j and k and a reference axis. The bond orientation correlation function is then defined as an average of the local bond orientation order,

$$g_6(r) = \frac{\left\langle \sum_{k \neq j}^N \Psi(r_j)^* \Psi(r_k) \delta(r - |r_j - r_k|) \right\rangle}{\left\langle \sum_{k \neq j}^N \delta(r - |r_j - r_k|) \right\rangle}. \quad (7)$$

A power-law decay of $g_6(r)$ means that there is a quasi-long-range orientation correlation. For the system in a hexatic phase, $g_6(r) \propto r^{-\eta}$, where $0 < \eta < 0.25$.

Liquid-solid transitions have been reported extensively in the literature for two-dimensional systems in lattice gas models with extended exclusion ranges. However, here our simulation results reveal a liquid-hexatic-solid phase transitions for the triangular lattice cover seven sites, which have the same nature of the phase transition as the melting transition of hard-disk molecules. Although melting is studied extensively in the literature,^{9,10} there is still controversy about the nature of its phase transition that can arise from the finite size effect or inefficiency of the system to equilibrate the system. In two-dimensional systems, there are three different scenarios for the melting transition of hard disks in the literature:

- Kosterlitz, Thouless, Halperin, Nelson, and Young (KTHNY) scenario:^{61–63} a two-step continuous phase transition, first from the liquid to hexatic phase and then from the hexatic to solid phase,^{64,65}
- Two step transition: first order phase transition from the liquid to hexatic phase and then continuous phase transition from the hexatic to solid phase,^{9,10}
- First order phase transition from the liquid to solid phase.⁶⁶

We will show in Sec. III how finite size effects and access to the thermodynamic regimes can bring uncertainty regarding phase behavior of the system, mainly the nature of phase transition where these issues are extensively reported in the literature about the nature of melting transition.^{9,67}

II. SIMULATION DETAILS

The adsorption of hard-core molecules with a third neighbor exclusion range on the triangular lattice involves the adsorption of molecules covering 7 adsorption sites in the manner as represented by a red circle in Fig. 1. As it is clear from the hexagon drawn around the adsorbate (red circle) in Figs. 1(a) and 1(b), this model could have two different orientations at high coverage in comparison with other adsorbates such as hard-core molecule with first neighbor exclusion.⁵⁴ Here, we employ two complementary methods as in our previous work:⁵⁴ an “adsorption method,” which begins from an empty lattice, and a “desorption method,” which begins with a full lattice and progressively decreases coverage. The results are expected to bracket the correct equilibrium equation of state.

In the adsorption method, molecules or particles are progressively added to an initially empty $d \times d$ lattice surface where a periodic boundary condition is used to ameliorate finite size effects. The only restriction is that overlap is not allowed; an assumption based physically on short-range electrostatic repulsion. For each adsorption attempt, a random position (x, y) is selected representing the center of mass of the particle. If the selected site and its neighbors are empty, adsorption is accepted. Otherwise, it is rejected. Diffusion, the simultaneous movement of particles, is introduced sequentially with a predefined ratio D between the number of diffusion attempts and the adsorption attempts: For $D = 3$, each adsorption is followed by 3 diffusion attempts, etc. For each diffusion attempt, a previously adsorbed particle and a direction for the displacement of the particle are selected randomly; an arrow in Fig. 1 illustrates the possible direction. If moving the center of the mass of the particle to the next node along this direction does not infringe the nonoverlap condition, diffusion is accepted. Otherwise, it is rejected. In the RSAD model, when diffusion is fast enough, the surface layer is at internal equilibrium (even during transient adsorption) and the blocking function can be considered as a state function.

For the desorption method, the lattice is initially full. For each simulation step, two particles are randomly selected and removed. Then, one adsorption attempt and D diffusion attempts are

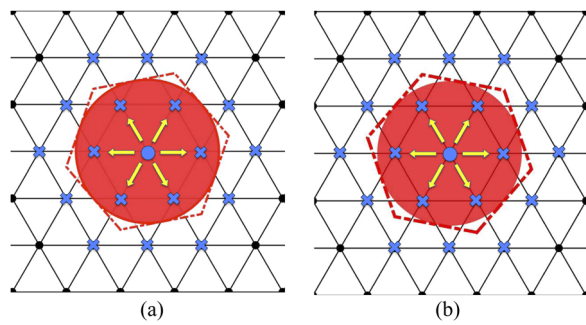


FIG. 1. Triangular lattice with first, second, and third neighbor exclusion where each adsorbate covers 7 sites. The center of the adsorbate is represented by a circle, arrows indicate possible displacements of particles, and stars represent the sites where the center of other particles is not allowed to adsorb. (a) and (b) show two different configurations at the maximum close packing.

performed following the same procedure as for the adsorption method. The choice of the sequence (2 desorption events followed by 1 adsorption) is arbitrary but answers the need at each time step to decrease coverage and add at least one particle to calculate the blocking function.

For both adsorption and desorption methods, the blocking function is extracted from the success rate of adsorption attempts. 500 runs are performed, and an ensemble average is used to reduce the noise arising from the numerical calculation of the derivative of the coverage. The blocking function is fitted with a polynomial function before it is used to generate the adsorption isotherm. The latter is inserted into the Gibbs adsorption isotherm equation to obtain the equation of state.

In this work, we also used a relaxation method in order to track the structure of particles by time and prove our hypothesis about expecting the correct equilibrium equation of state starting from either the adsorption or the desorption method. In this method, either the adsorption or the desorption method can be used to reach a specific coverage. In the second step, one adsorption attempt and D diffusion attempts are performed following the same procedure as for the adsorption method. In order to keep the coverage constant, if the adsorption attempt is successful, one particle is randomly selected and removed. 1500 runs are performed to extract the success rate of adsorption attempts or, in other words, the blocking function.

III. RESULTS

Accessing the thermodynamic regime is an initial step toward studying the phase behavior of the system^{9,10} where some algorithms are insufficient to equilibrate the system in order to study the phase transition of the system in a reliable manner.⁶⁴ The effect of surface diffusion for a lattice size $d = 105$ is studied in Fig. 2. Initially, when the system is diluted, all of the curves regardless of their methods or their surface diffusion overlap in the low surface coverage, as presented in Fig. 2(a). The fluctuation in the phase transition region is much larger than the pure liquid and solid phase, where the difference is maximized in the middle of phase transition, as illustrated in Fig. 2(b).⁶⁶ As presented in Fig. 2(b), at high surface coverage, probability of success of adsorbing a new particle initially decreases due to the caging effect. However, by increasing the ordering of particles, this caging effect will be diminished in order to maximize the available surface for accepting the new incoming particles. The system reaches the equilibrium state when two curves overlap in the whole range of fractional surface coverage, so accessing the thermodynamic regime will be apparent.

Figure 3 represents the relaxation of blocking function of hard-core molecules with third neighbor exclusion on a triangular lattice for $D = 0.01$, $d = 196$, and $\theta = 0.915$. This figure confirms that the equilibrium state is a function of a blocking function and does not depend on initial configuration. The blocking function of the desorption method increases in time until it reaches the equilibrium value, whereas the adsorption method shows the opposite trend. Simulation data show that the desorption method reaches the equilibrium value faster than the adsorption method.

Finite size effects are another important key issue in finding the equation of state in lattice simulations. Figure 4 presents the

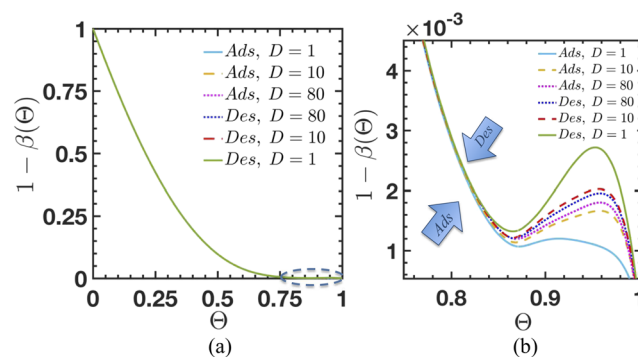


FIG. 2. (a) Effect of surface diffusion on the adsorption rate vs surface coverage for $d = 105$. Ads and Des refer to adsorption and desorption methods, respectively. (b) The inset expands the high-coverage region where sensitivity to surface diffusion appears.

variation in the adsorption rate for triangular lattices covering 7 sites of sizes 105–266. For surface diffusion of $D = 1$, the same blocking function is obtained from both adsorption and desorption methods at low surface coverage, as presented in Fig. 4(a). Initially, in the vicinity of the phase transition, by increasing the lattice size dimension, the adsorption rate increases for both the adsorption and desorption methods, as illustrated in Fig. 4(b). Exactly before all of the curves overlap around full coverage, the adsorption rate decreases by increasing the lattice dimension for both methods. The results in Fig. 4(b) show that the adsorption rate is significantly different for $d = 105$ in comparison with $d = 196$ and $d = 266$. As a result, $d = 105$ is not a reliable lattice size for finding the equation of state. Later on, we will discuss this case and compare it with $d = 196$ in Figs. 5(b) and 6 only to show the importance of using a large enough system. One of the advantages of using the RSAD method is we know how big our system should be to ensure that the results are, at the same time, accurate and computationally less expensive.

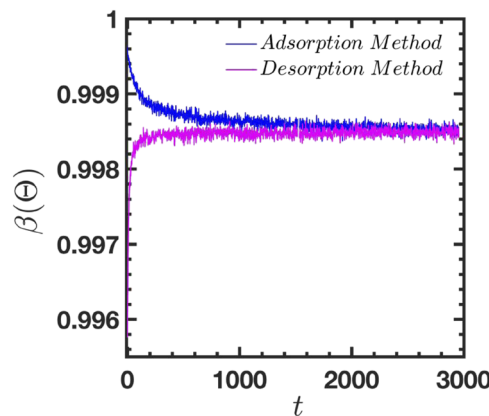


FIG. 3. Relaxation dynamics of a hard core molecule with third neighbor exclusion on a triangular lattice for a surface coverage of $\theta = 0.915$ and $d = 196$. $D = 0.01$ in both the first and second steps. Adsorption and desorption methods refer to the initial configuration to reach the surface coverage of 0.915.

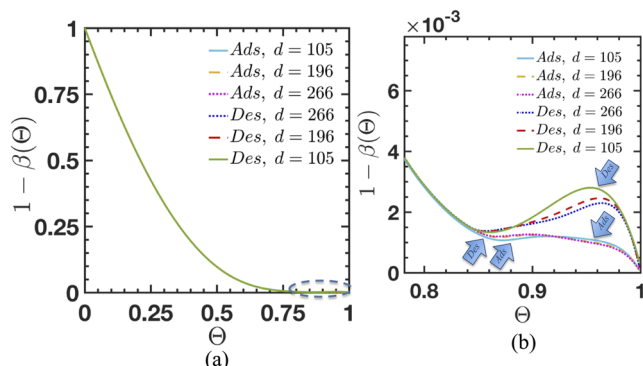


FIG. 4. (a) Effect of lattice size on the adsorption rate vs surface coverage for $D = 1$. Ads and Des refer to adsorption and desorption methods, respectively. (b) The inset expands the high-coverage region where sensitivity to lattice size appears.

Although an exact solution of this model does not exist in the literature, meaning that there is no certain agreement upon the equation of state and its phase transition, we can compare our results with the analytic calculation of Orban and Bellmans³³ for $d = 196$ and $D = 80$ in Fig. 5(a). This paper used two different methods, the matrix method, based on the sequence of exact solutions for lattices of infinite length and increasing finite width, and the series expansion method, based on knowing the final structure at close packing and constructing the density and activity series to find the surface pressure. A first order transition was found for both the matrix and the series expansion methods, where the transition occurs at surface pressure of 4.5–5 for surface coverages of 0.81 ± 3 and 0.98 ± 1 for fluid and solid regimes, respectively. This system is also studied by Chestnut³³ using a Monte Carlo technique, but the study was limited to surface coverages lower than 0.75, where no phase transition was found.

As illustrated in Fig. 5(a), at low surface coverage, there is no difference between the reported equations of state. However, in the

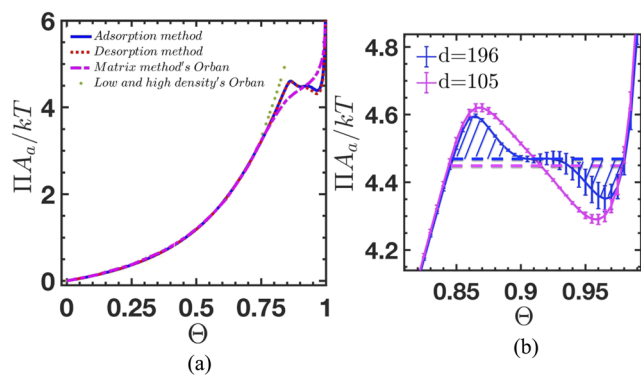


FIG. 5. (a) Comparison of our EOS where $d = 196$ and $D = 80$ with Orban and Bellman (matrix method and low and high density method)³³ for hard core molecules on a triangular lattice covers 7 sites. (b) The inset shows a magnified view of error bar between the adsorption and desorption method for $(d = 196, D = 80)$ and $(d = 105, D = 80)$ in the phase transition region.

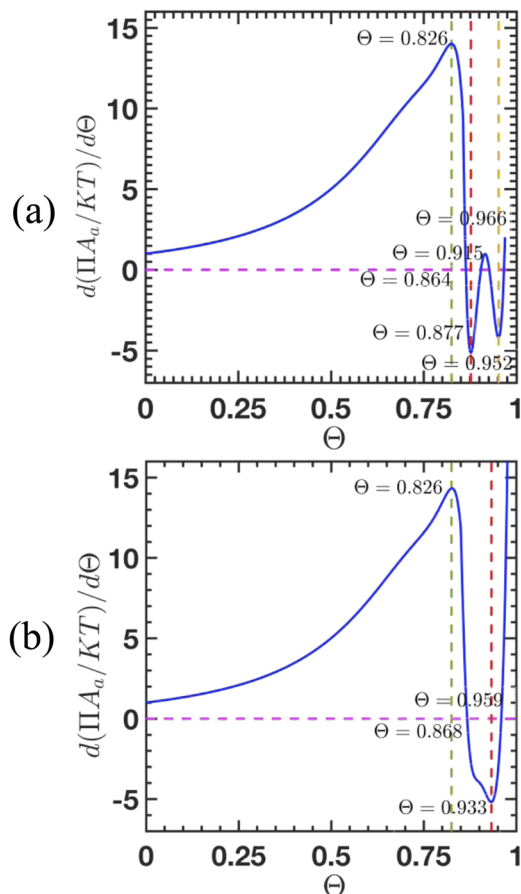


FIG. 6. (a) Analysis of the phase transition region where $d = 196$ and $D = 80$ and (b) $d = 105$ and $D = 80$.

lower part of the phase transition zone, our equation of states shows lower surface pressure than Orban and Bellman's series expansion method (low and high density) but higher surface pressure than their matrix method. On the contrary, in the upper part of the phase transition region, the matrix method shows higher surface pressure than what we found, but the series expansion method overlaps with both of our methods. The thermodynamically stable surface pressure loop is observed in our simulation results as is reported extensively in the literature due to finite size effects.^{9,10,68,69} Surface pressure can create a thermodynamically stable loop at equilibrium for a finite size system, but this loop will disappear at infinite size and the coexistence zone will be flat. Creation of the flat pressure is visible in Fig. 5(b) for $d = 196$ around a surface pressure of 4.5 ± 0.05 . Moreover, based on the lower part of the phase transition in Fig. 4(b), the adsorption rate tends to increase by increasing the lattice dimension, which means less surface pressure will be expected for a larger lattice size. Conversely, the adsorption rate tends to decrease for both the adsorption and desorption methods in the upper part of the phase transition, which means higher surface pressure will be expected for a larger lattice size. This behavior indicates the tendency of the system toward flatness at an infinite size. From the equality shown in the hatched

area of Fig. 5(b), the horizontal surface pressure is obtained from the Maxwell construction, where overlapping of this construction line with the flat region of the equation of state confirms the tendency of the system to be flat at infinite size. Fig. 5(b) shows that by increasing the lattice dimension, surface pressure decreases in the lower part of the phase transition and increases in the upper part of phase transition. Bernard *et al.*^{9,10} reported the same trend for the equation of state of the melting transition of hard disks by increasing the number of particles where they reported a two step transition, first order liquid-hexatic and continuous hexatic-solid transition for their system.

The phase transition zone is studied in Fig. 6 based on the derivative of surface pressure with respect to surface coverage in the adsorption method. One can see from Fig. 6(b) that for an insufficiently large system, the first order liquid-solid phase transition is obtained for $d = 105$ and $D = 80$; however, a different phase

transition is obtained for $d = 196$ and $D = 80$ in Fig. 6(a), which indicates the importance of using a sufficiently large system. Phase transition peaks obtained from Fig. 6(a) for $d = 196$, $D = 80$ are analyzed through a bond orientation correlation function, $g_6(r)$, in Fig. 7 based on the relaxation method for each individual configuration. For additional insight into the phase transition region, each of these configurations is visualized via the local bond orientation order function $\Psi(r)$, based on the relaxation method, in Fig. 8. The first peak in the phase transition curve corresponds to a surface coverage of 0.826. The fact that the same exponential decay of $g_6(r)$ before and after relaxation at a surface coverage of 0.75 [see Fig. 7(a)] suggests that the system is in a pure liquid regime below a surface coverage of 0.826. Furthermore, the homogeneous distribution of local bond orientation order over the surface in Fig. 8(a) confirms the presence of a liquid phase below a surface coverage of 0.826. In Fig. 6, we see that lattice size does not have any impact on the liquid

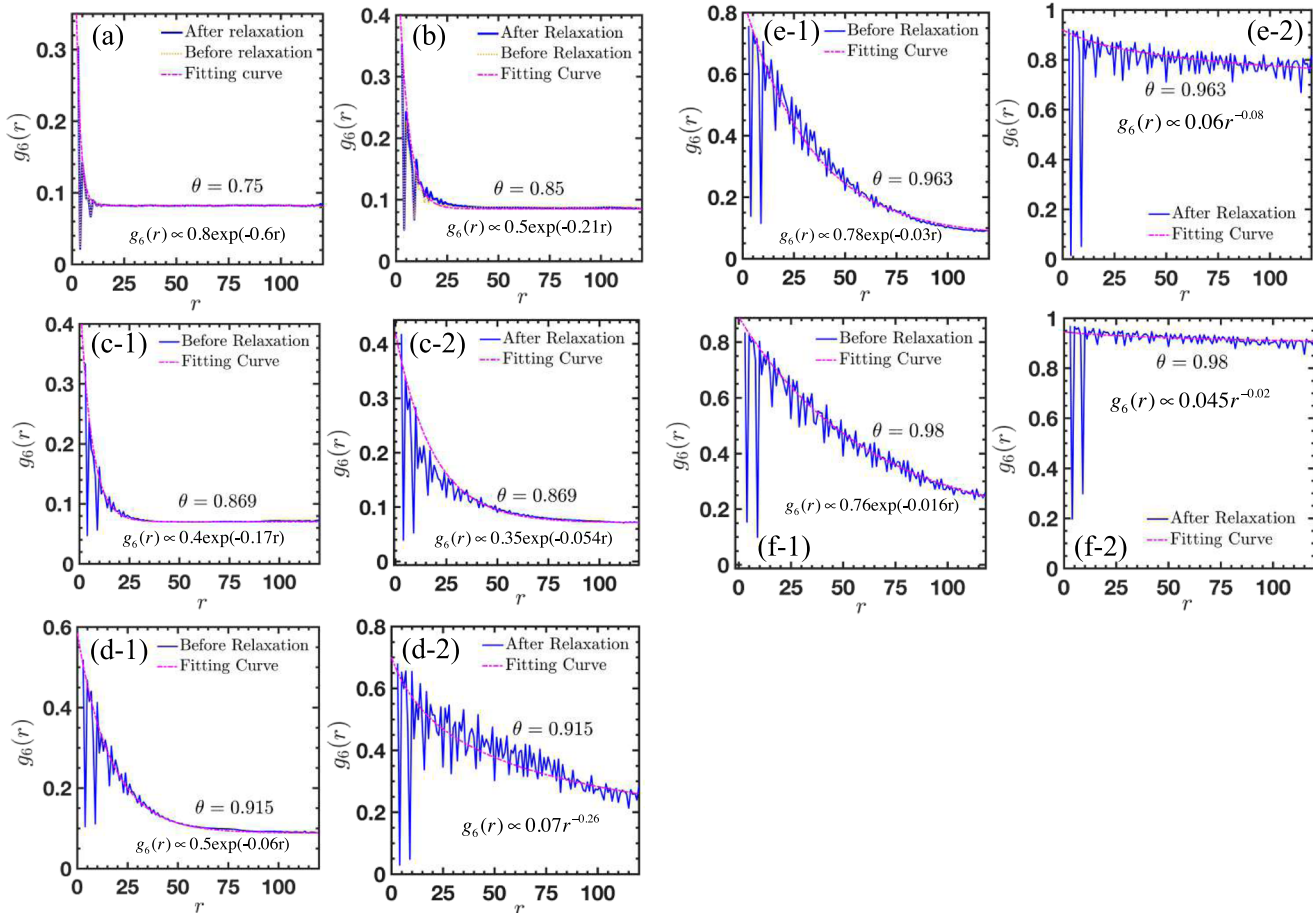


FIG. 7. Bond orientation correlation function of the hard core molecule with third neighbor exclusion based on the relaxation method, where $d = 196$ and $D = 0.01$ in both steps of relaxation at different surface coverages: (a) $\theta = 0.75$, (b) $\theta = 0.85$, (c-1) and (c-2) $\theta = 0.869$, (d-1) and (d-2) $\theta = 0.915$, (e-1) and (e-2) $\theta = 0.963$, and (f-1) and (f-2) $\theta = 0.98$. Before relaxation refers to the configuration obtained from the adsorption method at $D = 0.01$ in the first step of the relaxation method, and after relaxation refers to the equilibrium configuration.

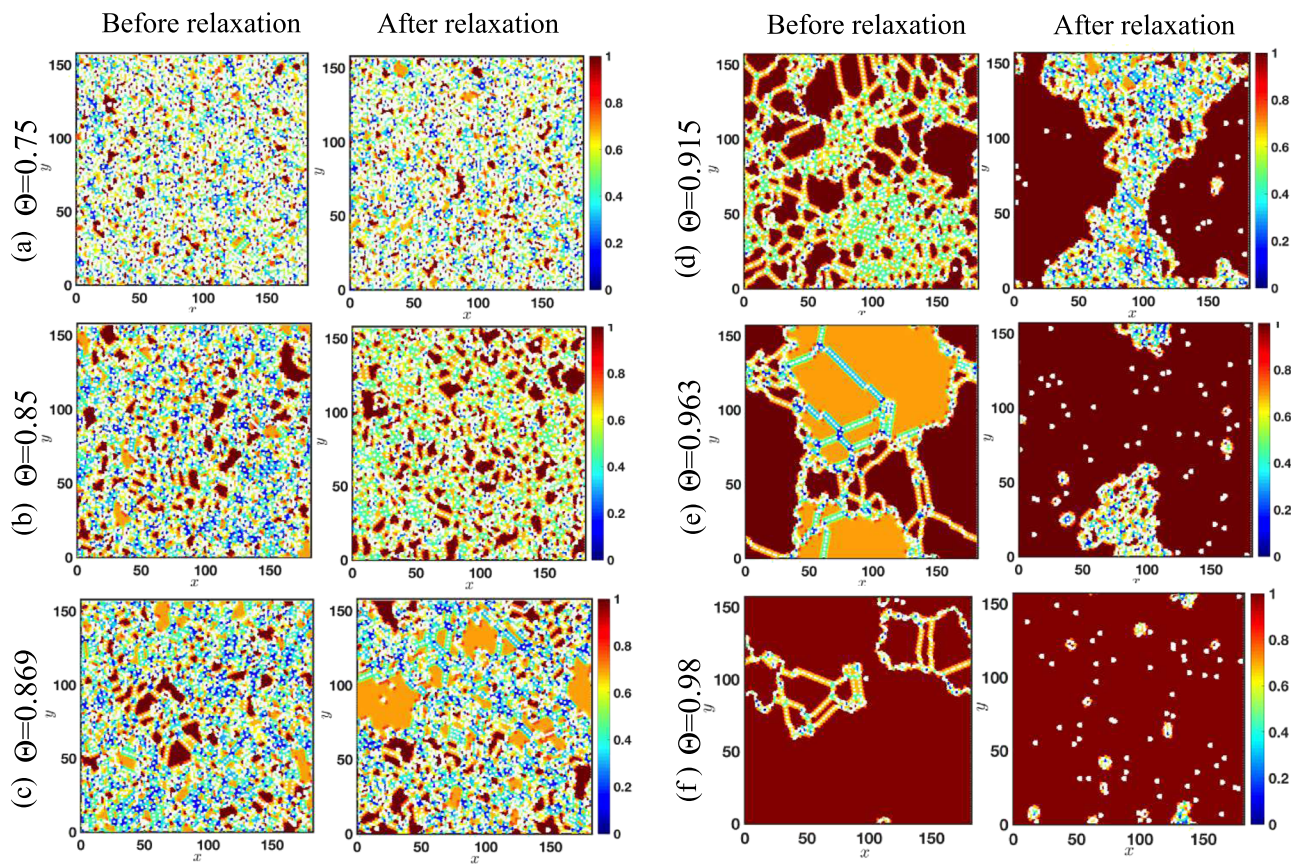


FIG. 8. Local bond orientation order based on the relaxation method at low surface diffusion $D = 0.01$ and different surface coverages: (a) $\theta = 0.75$, (b) $\theta = 0.85$, (c) $\theta = 0.869$, (d) $\theta = 0.915$, (e) $\theta = 0.963$, and (f) $\theta = 0.98$. Before relaxation refers to the configuration obtained from the adsorption method at $D = 0.01$ in the first step of the relaxation method, and after relaxation refers to the equilibrium configuration.

phase since the same behavior from the liquid regime is obtained for both $d = 105$ and $d = 196$ through fractional surface coverage up to 0.826.

The transition between positive and negative slopes occurs at a surface coverage of 0.864, located between the first and second peaks, so we analyze surface coverages of 0.85 and 0.869 to see the behavior of the system below and above the transition value. For a surface coverage of 0.85, $g_6(r)$ decays exponentially at the same rate before and after relaxation in Fig. 7(b); more peaks were observed after relaxation, which is an indication of the creation of a more ordered phase in the system. Creation of a more ordered phase is also confirmed by the local bond orientation order seen in Fig. 8(b), indicated by more red spread through the surface. For a surface coverage of 0.869, $g_6(r)$ still decays exponentially but at different rates before and after relaxation, as illustrated in Figs. 7(c-1) and (c-2), respectively. The local bond orientation order in Fig. 8(c) shows that ordered particles prefer to stick to each other. The third peak in Fig. 6 corresponds to a surface coverage of 0.915. At this coverage, the system decays exponentially before relaxation, as presented in Figs. 7(d-1) and 8(d) shows that the cluster of the ordered phase spreads through the surface and indicates a glassy state. After relaxation, $g_6(r)$ decays with

a power law with $\theta = 0.25$, as illustrated in Fig. 7(d-2), which is an indication of a hexatic phase. The local bond orientation order shown in Fig. 8(d) reveals that at this coverage, all the ordered particles tend to stick together and they are between the mobile particles, as was also reported in Ref. 3. The tendency of ordered particles to stick together causes the probability of success to increase in Fig. 2(b) due to maximizing the available free surface for accepting the new incoming particles. By increasing the surface coverage from 0.915 to 0.963, η decreases from 0.25 to 0.08 after relaxation, as illustrated in Fig. 7(e-2), which indicates that the fourth peak in Fig. 6 corresponds to a first order transition from the hexatic phase to solid phase in the equilibrium state.

To further illustrate the relaxation dynamics toward an equilibrium state, the local bond orientation order parameter of particles at a surface coverage of 0.915 was tracked over time for two different initial configurations obtained from adsorption and desorption methods at very low surface diffusion ($D = 0.01$, $d = 196$). Figure 9(a) indicates that the density should be increased very slowly when we start from an empty lattice, or else the system will be locked into a glassy configuration.⁶⁶ A glassy state is reported in Ref. 3 during rapid compression of a system composed of spherical particles. For

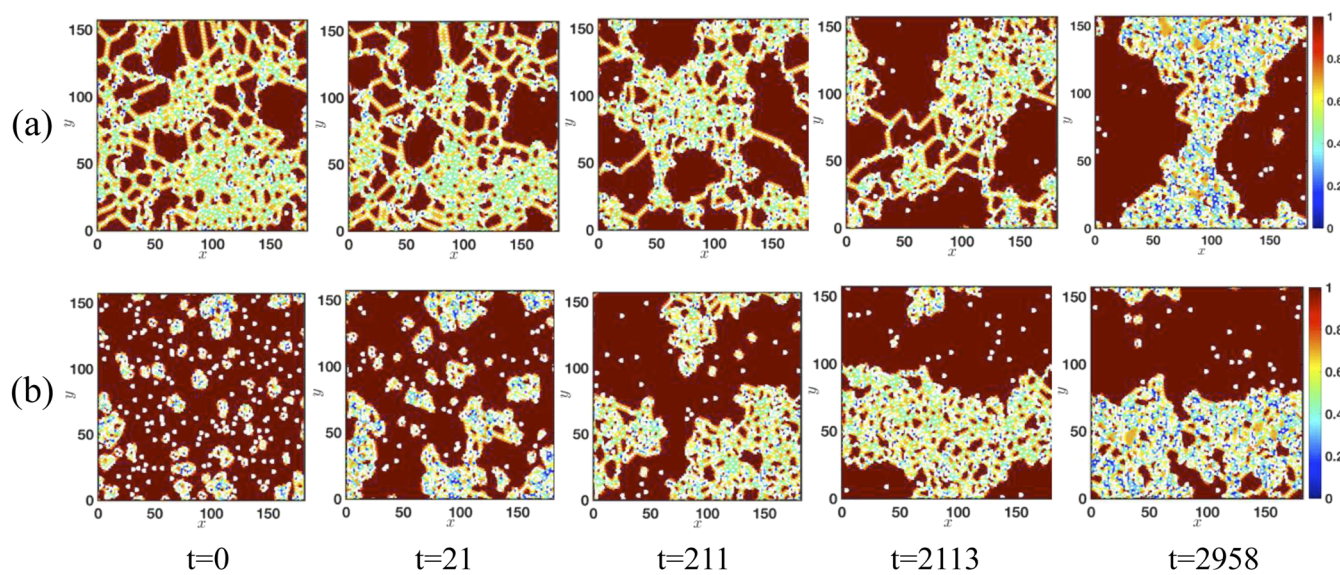


FIG. 9. Local bond orientation order for a surface coverage of 0.915 with $D = 0.01$ and $d = 196$: (a) for adsorption method over time and (b) for desorption method over time.

the desorption method [Fig. 9(b)], the system is initially ordered, so the density should be decreased very slowly or else the system will be metastable.⁶⁶ As time passes in the equilibrium state, phase separation occurs, where ordered particles tend to cluster and create more space for further adsorption.

IV. CONCLUSION

In this paper, we studied the phase behavior of hard-core molecules with third neighbor exclusions in a triangular lattice with RSAD simulations, in order to derive the equation of state of a two-dimensional hard-core particle based on kinetic arguments and the Gibbs adsorption isotherm. We compared our results with the result of Orban and Bellman,³³ who used a matrix method and a series expansion method in low and high densities, and found only partial agreement. Our results show that the system is in a pure liquid regime below a surface coverage of 0.826. Increasing the surface coverage will create a more ordered phase where a first order liquid-hexatic phase transition occurs between surface coverages of 0.877 and 0.915. At a surface coverage of 0.915, $g_6(r)$ decays algebraically after relaxation with a power-law exponent $\eta = 0.25$, which is an indication of a hexatic phase. Our simulation results reveal that as the surface coverage increases, after relaxation, the surface particles tend to form tightly packed clusters in like-oriented domains, while the remaining mobile particles have more random orientations. By increasing the surface coverage above 0.915, η decreases from 0.25 toward zero after relaxation, where the system undergoes a first order transition from a hexatic phase to a solid phase.

One of the advantages of using the RSAD model is being able to locate the equilibrium state, which assures us that adequate thermalization and finite size are being used to reach the equilibrium state. Moreover, subtle details of the clustering structure, through

direct visualization of the system using the relaxation method at any fractional surface coverage, provide insight regarding coexistence regions and phase transitions.

ACKNOWLEDGMENTS

This research was supported by the National Science Foundation under Grant No. 1743794, PIRE: Investigation of Multi-Scale, Multi-Phase Phenomena in Complex Fluids for the Energy Industries.

REFERENCES

- V. Pauchard, J. P. Rane, and S. Banerjee, "Asphaltenes-laden interfaces form soft glassy layers in contraction experiments: A mechanism for coalescence blocking," *Langmuir* **30**, 12795–12803 (2014).
- F. Liu, S. Darjani, N. Akhmetkhanova, C. Maldarelli, S. Banerjee, and V. Pauchard, "Mixture effect on the dilatation rheology of asphaltenes-laden interfaces," *Langmuir* **33**, 1927–1942 (2017).
- Z. Hou, K. Zhao, Y. Zong, and T. G. Mason, "Phase behavior of two-dimensional Brownian systems of corner-rounded hexagons," *Phys. Rev. Mater.* **3**, 015601 (2019).
- S. Fortuna, D. L. Cheung, and A. Troisi, "Hexagonal lattice model of the patterns formed by hydrogen-bonded molecules on the surface," *J. Phys. Chem. B* **114**, 1849–1858 (2010).
- U. K. Weber, V. M. Burlakov, L. M. A. Perdigao, R. H. J. Fawcett, P. H. Beton, N. R. Champness, J. H. Jefferson, G. A. D. Briggs, and D. G. Pettifor, "Role of interaction anisotropy in the formation and stability of molecular templates," *Phys. Rev. Lett.* **100**, 156101 (2008).
- V. A. Gorbunov, S. S. Akimenko, A. V. Myshlyavtsev, V. F. Fefelov, and M. D. Myshlyavtseva, "Adsorption of triangular-shaped molecules with directional nearest-neighbor interactions on a triangular lattice," *Adsorption* **19**, 571–580 (2013).
- P. Bak, P. Kleban, W. N. Unertl, J. Ochab, G. Akinci, N. C. Bartelt, and T. L. Einstein, "Phase diagram of selenium adsorbed on the Ni(100) surface: A physical realization of the Ashkin-Teller model," *Phys. Rev. Lett.* **54**, 1539 (1985).

⁸D. E. Taylor, E. D. Williams, R. L. Park, N. C. Bartelt, and T. L. Einstein, "Two-dimensional ordering of chlorine on Ag(100)," *Phys. Rev. B* **32**, 4653 (1985).

⁹E. P. Bernard and W. Krauth, "Two-step melting in two dimensions: First-order liquid-hexatic transition," *Phys. Rev. Lett.* **107**, 155704 (2011).

¹⁰M. Engel, J. A. Anderson, S. C. Glotzer, M. Isobe, E. P. Bernard, and W. Krauth, "Hard-disk equation of state: First-order liquid-hexatic transition in two dimensions with three simulation methods," *Phys. Rev. E* **87**, 042134 (2013).

¹¹I. Langmuir, "The adsorption of gases on plane surfaces of glass, mica and platinum," *J. Am. Chem. Soc.* **40**, 1361–1403 (1918).

¹²J. P. Rane, S. Zarkar, V. Pauchard, O. C. Mullins, D. Christie, A. B. Andrews, A. E. Pomerantz, and S. Banerjee, "Applicability of the Langmuir equation of state for asphaltene adsorption at the oil–water interface: Coal-derived, petroleum, and synthetic asphaltenes," *Energy Fuels* **29**, 3584–3590 (2015).

¹³J. P. Rane, V. Pauchard, A. Couzis, and S. Banerjee, "Interfacial rheology of asphaltenes at oil–water interfaces and interpretation of the equation of state," *Langmuir* **29**, 4750–4759 (2013).

¹⁴K. Y. Foo and B. H. Hameed, "Insights into the modeling of adsorption isotherm systems," *Chem. Eng. J.* **156**, 2–10 (2010).

¹⁵J.-S. Wang, P. Nielaba, and V. Privman, "Collective effects in random sequential adsorption of diffusing hard squares," *Mod. Phys. Lett. B* **7**, 189–196 (1993).

¹⁶B. M. Manzi, M. Werner, E. P. Ivanova, R. J. Crawford, and V. A. Baulin, "Simulations of protein adsorption on nanostructured surfaces," *Sci. Rep.* **9**, 4694 (2019).

¹⁷I. Lončarević, L. Budinski-Petković, S. B. Vrhovac, and A. Belić, "Adsorption, desorption, and diffusion of k -mers on a one-dimensional lattice," *Phys. Rev. E* **80**, 021115 (2009).

¹⁸I. Lončarević, L. Budinski-Petković, and S. B. Vrhovac, "Reversible random sequential adsorption of mixtures on a triangular lattice," *Phys. Rev. E* **76**, 031104 (2007).

¹⁹J. Talbot, G. Tarjus, P. R. Van Tassel, and P. Viot, "From car parking to protein adsorption: An overview of sequential adsorption processes," *Colloids Surf., A* **165**, 287–324 (2000).

²⁰J. W. Evans, "Random and cooperative sequential adsorption," *Rev. Mod. Phys.* **65**, 1281 (1993).

²¹P. L. Krapivsky and E. Ben-Naim, "Collective properties of adsorption–desorption processes," *J. Chem. Phys.* **100**, 6778–6782 (1994).

²²J.-S. Wang, P. Nielaba, and V. Privman, "Locally frozen defects in random sequential adsorption with diffusional relaxation," *Physica A* **199**, 527–538 (1993).

²³J. R. Šćepanović, D. Stojiljković, Z. M. Jakšić, L. Budinski-Petković, and S. B. Vrhovac, "Response properties in the adsorption–desorption model on a triangular lattice," *Physica A* **451**, 213–226 (2016).

²⁴G. Tarjus and P. Viot, "Statistical mechanical description of the parking-lot model for vibrated granular materials," *Phys. Rev. E* **69**, 011307 (2004).

²⁵M. A. Meineke and J. D. Gezelter, "Random sequential adsorption model for the differential coverage of gold (111) surfaces by two related silicon phthalocyanines," *J. Phys. Chem. B* **105**, 6515–6519 (2001).

²⁶P. Schaaf and J. Talbot, "Surface exclusion effects in adsorption processes," *J. Chem. Phys.* **91**, 4401–4409 (1989).

²⁷J. J. Ramsden, "Observation of anomalous diffusion of proteins near surfaces," *J. Phys. Chem.* **96**, 3388–3391 (1992).

²⁸S. Ji, C. Ates, and I. Lesanovsky, "Two-dimensional Rydberg gases and the quantum hard-squares model," *Phys. Rev. Lett.* **107**, 060406 (2011).

²⁹M. Lackinger, S. Griessl, T. Markert, F. Jamitzky, and W. M. Heckl, "Self-assembly of benzene- dicarboxylic acid isomers at the liquid solid interface: Steric aspects of hydrogen bonding," *J. Phys. Chem. B* **108**, 13652–13655 (2004).

³⁰Y. Zhang, V. Blum, and K. Reuter, "Accuracy of first-principles lateral interactions: Oxygen at Pd(100)," *Phys. Rev. B* **75**, 235406 (2007).

³¹R. J. Baxter, *Exactly Solved Models in Statistical Mechanics* (Elsevier, 2016).

³²A. Bellemans and R. K. Nigam, "Phase transitions in two-dimensional lattice gases of hard-square molecules," *J. Chem. Phys.* **46**, 2922–2935 (1967).

³³J. Orban and A. Bellemans, "Phase transitions in two-dimensional lattice gases of hard-core molecules. The triangular lattice," *J. Chem. Phys.* **49**, 363–370 (1968).

³⁴F. H. Ree and D. A. Chesnut, "Phase transition of a hard-core lattice gas. the square lattice with nearest-neighbor exclusion," *J. Chem. Phys.* **45**, 3983–4003 (1966).

³⁵L. K. Runnels, L. L. Combs, and J. P. Salvant, "Exact finite method of lattice statistics. II. Honeycomb-lattice gas of hard molecules," *J. Chem. Phys.* **47**, 4015–4020 (1967).

³⁶L. K. Runnels and L. L. Combs, "Exact finite method of lattice statistics. I. Square and triangular lattice gases of hard molecules," *J. Chem. Phys.* **45**, 2482–2492 (1966).

³⁷X. Feng, H. W. J. Blöte, and B. Nienhuis, "Lattice gas with nearest-and next-to-nearest-neighbor exclusion," *Phys. Rev. E* **83**, 061153 (2011).

³⁸Z. Rotman and E. Eisenberg, "Critical exponents from cluster coefficients," *Phys. Rev. E* **80**, 031126 (2009).

³⁹D. S. Gaunt and M. E. Fisher, "Hard-sphere lattice gases. I. Plane-square lattice," *J. Chem. Phys.* **43**, 2840–2863 (1965).

⁴⁰D. S. Gaunt, "Hard-sphere lattice gases. II. Plane-triangular and three-dimensional lattices," *J. Chem. Phys.* **46**, 3237–3259 (1967).

⁴¹E. Eisenberg and A. Baram, "A first-order phase transition and a super-cooled fluid in a two-dimensional lattice gas model," *EPL (Europhys. Lett.)* **71**, 900 (2005).

⁴²M. V. Ushcats, "High-density equation of state for a lattice gas," *Phys. Rev. E* **91**, 052144 (2015).

⁴³M. V. Ushcats, L. A. Bulavin, V. M. Syssoev, and S. J. Ushcats, "Virial and high-density expansions for the lee-yang lattice gas," *Phys. Rev. E* **94**, 012143 (2016).

⁴⁴E. R. Cowley, "A Bethe model for phase transitions in the hard sphere lattice gas," *J. Chem. Phys.* **71**, 458–461 (1979).

⁴⁵D. M. Burley, "A lattice model of a classical hard sphere gas," *Proc. Phys. Soc.* **75**, 262 (1960).

⁴⁶H. Hansen-Goos and W. Martin, "A hard-sphere model on generalized Bethe lattices: Statics," *J. Stat. Mech.: Theory Exp.* **2005**, P04006.

⁴⁷K. Binder and D. P. Landau, "Phase diagrams and critical behavior in Ising square lattices with nearest-and next-nearest-neighbor interactions," *Phys. Rev. B* **21**, 1941 (1980).

⁴⁸D. A. Chesnut, "A Monte Carlo study of the thermodynamic properties of 'hard hexagons' on the triangular lattice," *J. Comput. Phys.* **7**, 409–434 (1971).

⁴⁹Da-J. Liu and J. W. Evans, "Ordering and percolation transitions for hard squares: Equilibrium versus nonequilibrium models for adsorbed layers with c (2×2) superlattice ordering," *Phys. Rev. B* **62**, 2134 (2000).

⁵⁰H. C. Marques Fernandes, J. J. Arenzon, and Y. Levin, "Monte Carlo simulations of two-dimensional hard core lattice gases," *J. Chem. Phys.* **126**, 114508 (2007).

⁵¹T. Nath and R. Rajesh, "Multiple phase transitions in extended hard-core lattice gas models in two dimensions," *Phys. Rev. E* **90**, 012120 (2014).

⁵²G. S. Rushbrooke and H. I. Scoins, "On the Ising problem and Mayer's cluster sums," *Proc. R. Soc. London, Ser. A* **230**, 74–90 (1955).

⁵³L. Lafuente and J. A. Cuesta, "Density functional theory for nearest-neighbor exclusion lattice gases in two and three dimensions," *Phys. Rev. E* **68**, 066120 (2003).

⁵⁴S. Darjani, J. Koplik, and V. Pauchard, "Extracting the equation of state of lattice gases from random sequential adsorption simulations by means of the Gibbs adsorption isotherm," *Phys. Rev. E* **96**, 052803 (2017).

⁵⁵H. C. Marques Fernandes, Y. Levin, and J. J. Arenzon, "Equation of state for hard-square lattice gases," *Phys. Rev. E* **75**, 052101 (2007).

⁵⁶L. Lafuente and J. A. Cuesta, "Phase behavior of hard-core lattice gases: A fundamental measure approach," *J. Chem. Phys.* **119**, 10832–10843 (2003).

⁵⁷K. Ramola and D. Dhar, "A high density perturbation expansion for the hard square lattice gas," in *AIP Conference Proceedings* (AIP, 2012), Vol. 1447, pp. 135–136.

⁵⁸D. Mandal, T. Nath, and R. Rajesh, "Estimating the critical parameters of the hard square lattice gas model," *J. Stat. Mech.: Theory Exp.* **2017**, 043201.

⁵⁹T. Nath and R. Rajesh, "The high density phase of the k -NN hard core lattice gas model," *J. Stat. Mech.: Theory Exp.* **2016**, 073203.

⁶⁰Da-J. Liu and J. W. Evans, "Lattice-gas modeling of the formation and ordering of oxygen adlayers on Pd(100)," *Surf. Sci.* **563**, 13–26 (2004).

⁶¹A. P. Young, "Melting and the vector coulomb gas in two dimensions," *Phys. Rev. B* **19**, 1855 (1979).

⁶²D. R. Nelson and B. I. Halperin, "Dislocation-mediated melting in two dimensions," *Phys. Rev. B* **19**, 2457 (1979).

⁶³J. M. Kosterlitz and D. J. Thouless, "Ordering, metastability and phase transitions in two-dimensional systems," *J. Phys. C: Solid State Phys.* **6**, 1181 (1973).

⁶⁴C. H. Mak, "Large-scale simulations of the two-dimensional melting of hard disks," *Phys. Rev. E* **73**, 065104 (2006).

⁶⁵Y. Peng, Z. Wang, A. M. Alsayed, A. G. Yodh, and Y. Han, "Melting of colloidal crystal films," *Phys. Rev. Lett.* **104**, 205703 (2010).

⁶⁶B. J. Alder and T. E. Wainwright, "Phase transition in elastic disks," *Phys. Rev.* **127**, 359 (1962).

⁶⁷K. Wierschem and E. Manousakis, "Simulation of melting of two-dimensional Lennard-Jones solids," *Phys. Rev. B* **83**, 214108 (2011).

⁶⁸J. E. Mayer and W. W. Wood, "Interfacial tension effects in finite, periodic, two-dimensional systems," *J. Chem. Phys.* **42**, 4268–4274 (1965).

⁶⁹M. Schrader, P. Virnau, and K. Binder, "Simulation of vapor-liquid coexistence in finite volumes: A method to compute the surface free energy of droplets," *Phys. Rev. E* **79**, 061104 (2009).